

# Phase transformations of amorphous semiconductor alloys under high pressures

V E Antonov, O I Barkalov, V K Fedotov, A I Harkunov and  
E G Ponyatovsky

Institute of Solid State Physics, RAS, 142432 Chernogolovka, Moscow District, Russia

Received 1 June 2002

Published 25 October 2002

Online at [stacks.iop.org/JPhysCM/14/11213](http://stacks.iop.org/JPhysCM/14/11213)

## Abstract

The paper reviews the results of experimental studies and thermodynamical modelling of metastable  $T$ – $P$  diagrams of initially amorphous GaSb–Ge and Zn–Sb alloys which provide a new insight into the problem of pressure-induced amorphization.

## 1. Introduction

Among the methods of solid-state amorphization, spontaneous amorphization of quenched high-pressure phases during their heating at ambient pressure is one of the most advantageous for producing bulk homogeneous samples. The first observations of this phenomenon were by McDonald *et al* [1] for the GaSb compound in 1965 and then independently by Belash and Ponyatovsky [2] for the Zn–Sb alloys in 1977. In the past few decades, amorphization of solids resulting from thermobaric treatments at temperatures below that of the glass transition has drawn the attention of many researchers, and it has been observed in various systems and for various treatments (while increasing and decreasing static pressures, in shock waves, upon deformation under pressure, etc). A lot of works have been devoted also to phase transformations in initially amorphous substances prepared by various techniques and subjected to high pressure at room temperature [3, 4].

The present paper will briefly review and discuss the results of our investigations on phase transformations occurring in the amorphous semiconductors GaSb–Ge [5] and Zn–Sb [6, 7] under high pressure at room and elevated temperatures up to 350 °C. The analysis of stable and metastable equilibria in the extended temperature range resulted in a new approach to amorphization in these and many other substances (Ge, Si, C, GaSb, Cd–Sb, etc), characterized by a decrease in the melting temperature of the crystalline low-pressure phase with increasing pressure.

## 2. The (GaSb)<sub>38</sub>Ge<sub>24</sub> alloy [5]

### 2.1. The experimental $T$ – $P$ diagram

The (GaSb)<sub>38</sub>Ge<sub>24</sub> amorphous alloy shows the highest thermal stability among amorphous semiconductors produced by solid-state amorphization of high-pressure phases [8, 9]. We

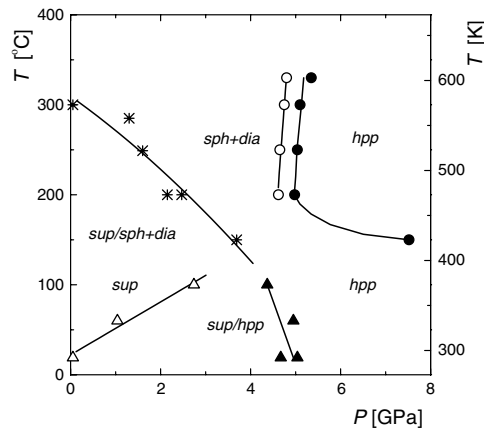


**Figure 1.** The  $T$ – $P$  diagram of phase transitions in the initially amorphous  $(\text{GaSb})_{38}\text{Ge}_{24}$ . The labels: sup = semiconductor unordered phase; hpp = high-pressure ‘ $\beta$ -Sn’-type phase; sph + dia = a mixture of the sphalerite-like and diamond-like low-pressure phases. The asterisks show the positions of the irreversible sup  $\rightarrow$  sph + dia transition at increasing temperature or pressure. The solid and open triangles stand for the sup  $\rightarrow$  hpp and hpp  $\rightarrow$  sup transitions at increasing and decreasing pressure, respectively. The solid and open circles indicate the sph + dia  $\rightarrow$  hpp and hpp  $\rightarrow$  sph + dia transitions, also at increasing and decreasing pressure. The labels with slashes mark the fields where either of the indicated phase compositions was possible depending on the previous treatment.

used it therefore as a model system. Figure 1 presents the  $T$ – $P$  phase diagram of this alloy constructed from the results of electrical resistance measurements and x-ray analyses of the samples quenched under pressure to 100 K.

At ambient pressure and temperatures below 630 °C, the equilibrium state of the  $(\text{GaSb})_{38}\text{Ge}_{24}$  alloy is a two-phase mixture of a GaSb-rich phase with a sphalerite-like structure and a Ge-rich phase with a diamond-like structure [10]. To prepare the starting amorphous  $(\text{GaSb})_{38}\text{Ge}_{24}$ , the sample was transformed to the single-phase high-pressure-phase (hpp) state of this composition by exposing it to 7.5 GPa and 250 °C, quenched to 100 K under pressure, and finally transformed to an amorphous state (semiconductor unordered phase sup) by heating at ambient pressure to 150 °C at a rate of 20 °C min<sup>−1</sup>. The neutron diffraction investigation showed [11] that amorphous  $(\text{GaSb})_{38}\text{Ge}_{24}$  thus prepared contains no crystalline inclusions.

Phase transformations in the samples never heated above 100 °C were qualitatively different from the transformations observed at higher temperatures. This allows one to consider the  $T$ – $P$  diagram in figure 1 as being composed of two separate parts, above and below 100 °C. The labelling of the fields in figure 1 takes account of this separation. The hpp that forms via a complex, multi-step sph + dia  $\rightarrow$  hpp transition at  $T > 150$  °C and the hpp formed from the metastable sup at  $T \leq 100$  °C and pressures exceeding 4.5–5 GPa are crystallographically identical. The sup  $\rightarrow$  hpp transition is reversible, and the pressure of amorphization of the hpp increases from nearly atmospheric at 17 °C to 2.7 GPa at 100 °C.

The  $T$ – $P$  diagram relevant for the discussion of the effect of pressure and temperature on phase transformations of a- $(\text{GaSb})_{38}\text{Ge}_{24}$  is actually the diagram of ‘isoconcentrational’ equilibria between the phases with a fixed composition of  $(\text{GaSb})_{38}\text{Ge}_{24}$ . In fact, the amorphous state is formed from and transforms to the phases with this composition only. At  $T \leq 100$  °C, such a phase is the hpp. At  $T > 100$  °C, a homogeneous sphalerite-like  $(\text{GaSb})_{38}\text{Ge}_{24}$  solid solution (low-pressure phase; lpp, hereafter) forms first as an intermediate metastable phase in the course of the sup crystallization to the thermodynamically equilibrium sph + dia mixture [9].

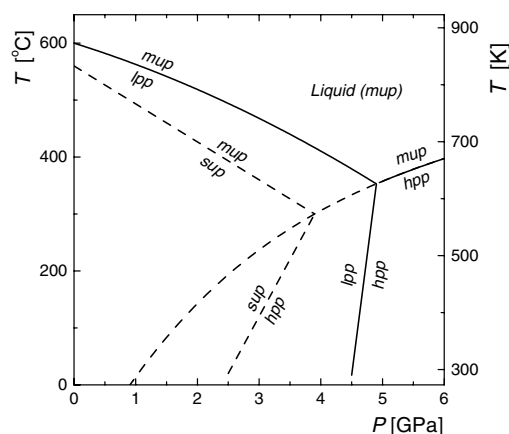


**Figure 2.** The  $T$ – $P$  diagram of metastable ‘isoconcentrational’ phase equilibria involving the lpp (solid curves) and the sup (dashed curves) of the  $(\text{GaSb})_{38}\text{Ge}_{24}$  alloy.

## 2.2. Metastable equilibria involving the lpp and sup

The metastable  $T$ – $P$  diagram of phase equilibria in the quasi-one-component  $(\text{GaSb})_{38}\text{Ge}_{24}$  system cannot be obtained directly in experiment. Nevertheless, it can be outlined rather reliably by interpolating  $T$ – $P$  diagrams [12] of GaSb and Ge and using the calculated [13] temperature  $T_0 = 600^\circ\text{C}$  of the ‘isoconcentrational’ melting of the  $(\text{GaSb})_{38}\text{Ge}_{24}$  lpp at ambient pressure. The diagram thus constructed is shown in figure 2 using solid curves. It is characterized by a triple point at around 5 GPa and  $350^\circ\text{C}$  of metastable equilibria among three phases, the lpp, the hpp, and the metallic liquid. The liquid is called a metallic unordered phase (mup) hereafter, so the same name can be used for this phase when it is in the equilibrium liquid state as well as in the undercooled liquid and amorphous states. The line of the lpp  $\leftrightarrow$  hpp equilibrium coincides well with the experimental sph + dia  $\leftrightarrow$  hpp line from figure 1.

The ‘isoconcentrational’ diagram of  $(\text{GaSb})_{38}\text{Ge}_{24}$  is thus an analogue of those [12] for Ge and GaSb. With a  $T$ – $P$  diagrams of this type, solid-state amorphization of the high-pressure phase is usually associated with the loss of its thermodynamic stability with respect to the long-range order when the phase crosses its extrapolated melting curve at a temperature which is low enough to suppress transformations to other crystalline modifications. This hypothesis of ‘cold melting’ was first formulated by Mishima *et al* [14]. Later the hypothesis of ‘cold melting’ as a cause of pressure-induced solid-state amorphization was adopted and widely used by many researchers including the authors of the present paper.

According to our DSC measurements, amorphization of the  $(\text{GaSb})_{38}\text{Ge}_{24}$  hpp at ambient pressure begins on heating to about  $-130^\circ\text{C}$ . To agree with the ‘cold-melting’ hypothesis, the melting curve of the hpp in figure 2 is extrapolated towards low pressures so as to cross the y-axis below this temperature.

As seen from figure 1, the sup  $\leftrightarrow$  hpp transformation in  $(\text{GaSb})_{38}\text{Ge}_{24}$  at  $T \leq 100^\circ\text{C}$  appears as a typical first-order phase transformation: it is reversible and exhibits a hysteresis decreasing with increasing temperature. This is possible only in the case where each of the final states of the transformation is a phase, i.e. the state corresponding to a minimum of the thermodynamic potential at given external parameters. The amorphous state in the  $(\text{GaSb})_{38}\text{Ge}_{24}$  system is thus a classic phase, though a metastable one, and not just a ‘frozen’ intermediate state.

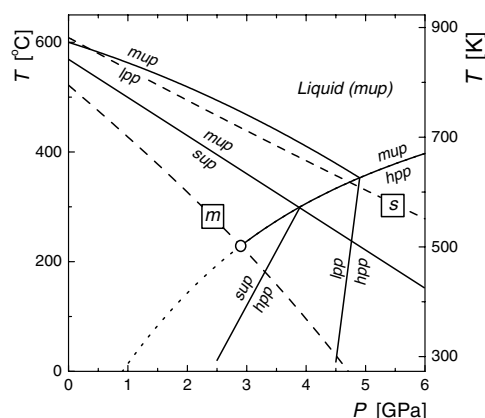


**Figure 3.** The  $T$ - $P$  diagram of metastable equilibria in the  $(\text{GaSb})_{38}\text{Ge}_{24}$  alloy. The dashed curves labelled 's' and 'm' show the boundaries of thermodynamic stability of the sup and mup, respectively. The open circle marks the pseudo-critical point.

As both sup and hpp are phases, the line of the  $\text{sup} \leftrightarrow \text{hpp}$  equilibrium should pass somewhere between the  $\text{sup} \rightarrow \text{hpp}$  and  $\text{hpp} \rightarrow \text{sup}$  lines in the  $T$ - $P$  diagram of  $(\text{GaSb})_{38}\text{Ge}_{24}$ . The available experimental data allow one to determine the position of this line more accurately.

The slope of an equilibrium line should follow the Clapeyron equation  $dT/dP = T \Delta V / \Delta H$ , where  $\Delta V$  and  $\Delta H$  are the differences between the volumes and enthalpies of the two phases in equilibrium at given  $T$  and  $P$  (if not specified, the temperature is in kelvins hereafter). With the room temperature experimental values of the integral heat of the  $\text{hpp} \rightarrow \text{sup}$  transition at ambient pressure of  $\Delta H^0 = +3.5 \text{ kJ mol}^{-1}$ , the pressure of the  $\text{sup} \leftrightarrow \text{hpp}$  equilibrium of  $P = 2.5 \text{ GPa}$  (this is the centre of the hysteresis interval at room temperature; see figure 1), and the volumes of  $V_{\text{sup}} = 16.3 \text{ cm}^3 \text{ mol}^{-1}$  and  $V_{\text{hpp}} = 13.2 \text{ cm}^3 \text{ mol}^{-1}$ , the Clapeyron equation gives  $dT/dP \approx +200 \text{ K GPa}^{-1}$ .

The  $\text{sup} \leftrightarrow \text{hpp}$  line with this slope is constructed in figure 2. As is seen, it intersects the  $\text{hpp} \leftrightarrow \text{mup}$  line at about 3.9 GPa and 570 K. In accordance with the phase rule, this intersection should be a triple point and give rise to a third line, the line of the  $\text{sup} \leftrightarrow \text{mup}$  equilibrium.

The line of the  $\text{sup} \leftrightarrow \text{mup}$  equilibrium is a new element for the  $T$ - $P$  diagrams with semiconductor amorphous phases. As a line of metastable equilibrium, it extends on both sides of the triple point (figure 3) and describes equilibrium between the sup and mup, which can be considered as liquid or solid (i.e. amorphous) phases depending on their viscosity at a given temperature. The  $\text{sup} \leftrightarrow \text{mup}$  line has never been observed in experiment, but its existence and approximate position were predicted for GaSb, InSb, and InAs compounds as a result of model calculations [15].

In the case of the  $(\text{GaSb})_{38}\text{Ge}_{24}$  system the position of the  $\text{sup} \leftrightarrow \text{mup}$  line can be determined rather accurately prior to model calculations. In fact, the slope of this line,  $dT/dP = T \Delta V / \Delta H = \Delta V / \Delta S$ , where  $S$  is the entropy, should be negative because  $\Delta S > 0$  and  $\Delta V < 0$  when any covalent substance melts to a metallic liquid [15, 16]. Moreover, the value of  $\Delta S$  should be of the order of  $30 \text{ J K}^{-1} \text{ mol}^{-1}$  if the substance is a covalent compound, and the value of  $\Delta V$  should not differ much from that for the  $\text{sup} \leftrightarrow \text{hpp}$  transformation [15]. This yields  $dT/dP$  of the order of  $-100 \text{ K GPa}^{-1}$ . The  $\text{sup} \leftrightarrow \text{mup}$  line with  $dT/dP = -100 \text{ K GPa}^{-1}$ , however, would intersect the  $\text{lpp} \leftrightarrow \text{mup}$  line at about 1.5 GPa. This does not look probable because it means that a metal-to-semiconductor transition should

occur in the  $(\text{GaSb})_{38}\text{Ge}_{24}$  melt at ambient pressure, whereas the melts of various diamond-like and sphalerite-like semiconductors studied at ambient pressure were shown to be metals with low concentrations of semiconductor clusters at all temperatures down to the melting point [17]. The sup  $\leftrightarrow$  mup line plotted in figure 3 has  $dT/dP = -70 \text{ K GPa}^{-1}$  which corresponds to  $\Delta S = 44 \text{ J K}^{-1} \text{ mol}^{-1}$ .

### 2.3. Model calculations

To find out more about the sup  $\leftrightarrow$  mup equilibrium, we used a simple two-level model which was first developed to describe the  $T$ – $P$  diagram of cerium undergoing an isomorphic transition [18] and then was successfully applied to the transitions between amorphous phases in ice [19] and GaSb, InSb, and InAs alloys [15]. The basic concept of this model assumes that both the mup and the sup consist of clusters of two types, metallic and semiconductor. These clusters are considered as two components of the unordered system, and the Gibbs potential,  $G(C)$ , is written in the approximation of regular solutions. However, by contrast to the standard approximation of regular solution, the concentration  $C$  of the metallic component is not an independent variable; its value is determined by the minimum conditions:  $\partial G/\partial C = 0$ ;  $\partial^2 G/\partial C^2 > 0$ .

As a function of  $C$ , the Gibbs potential can have one or two minima depending on the  $T$ – $P$  region. Two minimum values of  $G(C)$  are equal along a straight line, which represents the first-order phase transformation between the mup and sup and terminates in a critical point at  $T_{cr}$  where the two minima coincide. The points on the  $T$ – $P$  plane, where one of the two minima of  $G(C)$  degenerates to an inflection point, form two lines starting from the critical point. These are spinodals, or the lines of complete loss of thermodynamic stability of one of the phases.

The Gibbs potential thus constructed can be specified in a unique fashion by the values of four parameters:  $U$ ,  $\Delta V$ ,  $\Delta S$ , and  $\Delta E_0$ , where  $U = 2RT_{cr}$  is the mixing energy, while the other parameters are the differences between the volumes, entropies, and internal energies of the components. In the case of  $(\text{GaSb})_{38}\text{Ge}_{24}$ ,  $\Delta V$  is equal to  $3.1 \text{ cm}^3 \text{ mol}^{-1}$ , and  $\Delta E = 36.2 \text{ kJ mol}^{-1}$  and  $\Delta S = 44 \text{ J K}^{-1} \text{ mol}^{-1}$  can be determined from the position of the sup  $\leftrightarrow$  mup line shown in figure 3. The value of  $U = 19 \text{ kJ mol}^{-1}$  was chosen so that  $C = 92 \text{ vol\%}$  at ambient pressure and 873 K which is the point of ‘isoconcentrational’ melting of the hpp. This concentration of the metallic component was observed [17] at the melting temperature in liquid GaSb, the nearest analogue of  $(\text{GaSb})_{38}\text{Ge}_{24}$ .

With the chosen value of  $U$ , the line of the sup  $\leftrightarrow$  mup equilibrium terminates at a critical point at about 1140 K and a negative pressure of about  $-4.3 \text{ GPa}$ . The calculated spinodals are shown in figure 3 by the dashed curves. The sup is no longer a phase above the line labelled ‘s’ and the mup cannot exist below the line labelled ‘m’.

### 2.4. Position of the ‘m’-line and the effects caused by phase instability

From the position of the ‘m’-line it is clear why the quenched hpp does not transform to a metallic amorphous state on heating at ambient pressure: this state just does not correspond to any minimum of the thermodynamic potential at temperatures up to about 800 K.

The position of this line also explains why no amorphous state of  $(\text{GaSb})_{38}\text{Ge}_{24}$  has ever been obtained by quenching from the melt at ambient pressure: the metallic melt becomes unstable and inevitably transforms to some other state at a rather high temperature, above 800 K; the cooling rate slows down because of the heat release accompanying the transformation, and this allows crystallization of the alloy.



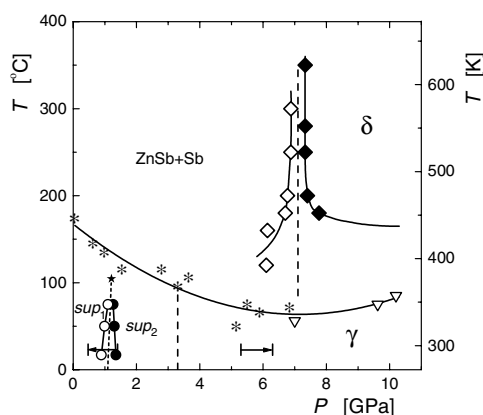


**Figure 5.** The  $T$ – $P$  diagram of phase transitions in the initially amorphous  $\text{Zn}_{41}\text{Sb}_{59}$  alloy.  $\text{sup}_1$  and  $\text{sup}_2$  are the low-pressure and high-pressure semiconductor unordered phases;  $\delta$  and  $\gamma$  are the stable and metastable crystalline phases. The right- and left-pointing arrows mark the pressure intervals of the  $\text{sup}_2 \rightarrow \gamma$  and  $\gamma \rightarrow \text{sup}_2$  transitions; the vertical dashed line at 3.3 GPa shows the tentative position of the line of the  $\text{sup}_2 \leftrightarrow \gamma$  metastable equilibrium. The asterisks indicate the positions of the irreversible transitions of the  $\text{sup}$  and  $\gamma$ -phases to a mixture of  $\text{ZnSb} + \text{Sb}$  at increasing temperature; the open triangles indicate the irreversible  $\gamma \rightarrow \delta$  transitions. The star marks the position of the critical point of the  $\text{sup}_1 \leftrightarrow \text{sup}_2$  equilibrium line.

determined by the line of the  $\text{hpp} \leftrightarrow \text{sup}$  equilibrium and not by the melting line of the  $\text{hpp}$  extrapolated from higher temperatures as was often thought before.

### 3. The $\text{Zn}_{41}\text{Sb}_{59}$ alloy [6, 7]

Similarly to the case for  $(\text{GaSb})_{38}\text{Ge}_{24}$ , the initial amorphous  $\text{Zn}_{41}\text{Sb}_{59}$  alloy was prepared from a high-pressure phase ( $\delta$ ) with a narrow range of composition, and the  $T$ – $P$  diagram presented in figure 5 was constructed using the same techniques. New elements of the  $\text{Zn}_{41}\text{Sb}_{59}$  diagram are the region of the metastable  $\gamma$ -phase, which irreversibly transforms to the  $\delta$ -phase on heating (triangles in figure 5), and the reversible first-order phase transition between two semiconductor amorphous phases,  $\text{sup}_1$  and  $\text{sup}_2$ , that occurs at around 1 GPa.

At room temperature, the  $\text{sup}_1 \rightarrow \text{sup}_2$  transition is accompanied by a 0.8% decrease in volume [21], and the  $\text{sup}_2$  remains amorphous up to the pressure of the  $\text{sup}_2 \leftrightarrow \gamma$  transition at about 6 GPa according to the *in situ* x-ray measurements in diamond anvils [6].

The temperature dependences of the pressures of the  $\text{sup}_1 \rightarrow \text{sup}_2$  and  $\text{sup}_2 \rightarrow \text{sup}_1$  transitions were determined using the electrical resistance measurement. The circles in figure 5 represent the positions of the steepest portions of the  $\log \rho(P)$  isotherms measured under hydrostatic conditions with increasing and decreasing pressure in steps of 0.1 GPa. At 17 and 50 °C, the sample was kept at each point until a tenfold decrease in the slope of the  $\log \rho$  versus time line was obtained, which took from 1 h at the edges of the pressure interval studied, of 0.4–1.7 GPa, to 15 h near the steepest portions of the  $\log \rho(P)$  dependences. At 75 °C, partial crystallization of the sample to a mixture of  $\text{ZnSb} + \text{Sb}$  contributed noticeably to the time dependence of  $\log \rho$ , and the 75 °C isotherm was measured in an isochronic regime, by holding the sample at each given pressure for 3 h.

From a structural point of view, the only difference between amorphous phases with the same composition, like those in  $\text{Zn}_{41}\text{Sb}_{59}$ , is their different short-range orders. Therefore, equilibria between such amorphous phases should be of the same type as those between

different phases in one-component liquids, which are considered as ‘liquid–liquid’ or ‘vapour–liquid’ equilibria depending on the density of the constituent phases. On the  $T$ – $P$  diagrams, the lines of these equilibria terminate either in a point of intersection with another equilibrium line or in a critical point. The behaviour of the electrical resistance of amorphous  $\text{Zn}_{41}\text{Sb}_{59}$  suggests that the line of the  $\text{sup}_1 \leftrightarrow \text{sup}_2$  equilibrium terminates in a critical point and that the critical temperature is of the order of  $100^\circ\text{C}$  as indicated by the star in figure 5.

In fact, the  $\text{sup}_1 \rightarrow \text{sup}_2$  and  $\text{sup}_2 \rightarrow \text{sup}_1$  transitions are very sluggish and no acceleration is observed with increase in temperature from  $17$  to  $75^\circ\text{C}$ . At the same time, the rate of crystallization to a mixture of  $\text{ZnSb} + \text{Sb}$  becomes noticeable at  $75^\circ\text{C}$ , though this process requires diffusion of atoms over much longer distances than in the course of the isoconcentrational  $\text{sup}_1 \leftrightarrow \text{sup}_2$  transformation. A significant decrease in the mobility of atoms is characteristic of systems approaching critical points. Therefore, the critical temperature of the  $\text{sup}_1 \leftrightarrow \text{sup}_2$  transformation should not be far above  $75^\circ\text{C}$ .

With kinetics of isomorphous phase transitions as sluggish as in the case of amorphous  $\text{Zn}_{41}\text{Sb}_{59}$ , one can expect the  $\text{sup}_1 \leftrightarrow \text{sup}_2$  transformation to exhibit a clearly visible hysteresis until the volume effect of this transformation is zero, i.e., until the critical temperature is reached. As is seen from figure 5, linear extrapolations of the lines of the  $\text{sup}_1 \rightarrow \text{sup}_2$  and  $\text{sup}_2 \rightarrow \text{sup}_1$  transitions give zero hysteresis at a temperature of about  $100^\circ\text{C}$ .

#### 4. Conclusions

The analysis of the available experimental data and the model calculations showed that amorphous  $(\text{GaSb})_{38}\text{Ge}_{24}$  is a metastable phase (not just a ‘frozen’ non-equilibrium intermediate state) and allowed construction of the  $T$ – $P$  diagram (figure 3) of metastable equilibria between this semiconductor unordered phase (sup), the crystalline high-pressure phase (hpp), and the metallic unordered phase (mup). In the diagram, both the sup and the mup can be considered as amorphous or liquid phases depending on their viscosity at a given temperature.

Amorphization of the  $(\text{GaSb})_{38}\text{Ge}_{24}$  hpp at decreasing pressure is shown to be thermodynamically possible under the conditions determined by the line of the  $\text{hpp} \leftrightarrow \text{sup}$  equilibrium and not by the melting curve of the hpp extrapolated from higher pressures, as was often thought before in similar cases. Moreover, the region where the mup can exist as a phase is bound from below (the ‘ $m$ ’-line in figure 3). The hpp melting curve terminates at a pseudo-critical point on intersection with this boundary and cannot be extended to lower temperatures.

The above features of amorphous  $(\text{GaSb})_{38}\text{Ge}_{24}$  are mainly determined by the topology of the  $T$ – $P$  diagram and should be characteristic of amorphous states formed at decreasing pressure in many systems with similar  $T$ – $P$  diagrams. The high-pressure investigation of amorphous  $\text{Zn}_{41}\text{Sb}_{59}$  demonstrated the possibility of a first-order phase transition between two different amorphous semiconductor phases. The  $T$ – $P$  diagram of  $\text{Zn}_{41}\text{Sb}_{59}$  (figure 5) is the first example of a diagram with a line of phase equilibrium between such phases.

#### Acknowledgments

One of the authors (VEA) thanks the Organizing Committee of AIRAPT-18 for financial support for attending the Conference. The support from the Russian Foundation for Basic Research under Grant No 99-02-17007 is also gratefully acknowledged.

## References

- [1] McDonald T R R *et al* 1965 *Science* **147** 1441
- [2] Belash I T and Ponyatovsky E G 1977 *High Temp.–High Pressures* **9** 651
- [3] Ponyatovsky E G and Barkalov O I 1992 *Mater. Sci. Rep.* **8** 147
- [4] Sharma S M and Sikka S K 1996 *Prog. Mater. Sci.* **40** 1
- [5] Antonov V E *et al* 1997 *High Pressure Res.* **15** 201
- [6] Antonov V E *et al* 2000 *Phys. Rev. B* **62** 3130
- [7] Antonov V E *et al* 2000 *High Pressure Res.* **17** 261
- [8] Sidorov V A *et al* 1994 *Phys. Rev. Lett.* **73** 3262
- [9] Brazhkin V V *et al* 1995 *J. Mater. Sci.* **30** 443
- [10] Panish M B 1966 *J. Electrochem. Soc.* **113** 626
- [11] Kolesnikov A I *et al* 2000 *Phys. Rev. B* **62** 9372
- [12] Tonkov E Yu 1992 *High Pressure Phase Transformations: a Handbook* (Philadelphia, PA: Gordon and Breach)
- [13] Ishihara K N *et al* 1988 *Mater. Trans. JIM Suppl.* **29** 249
- [14] Mishima O *et al* 1984 *Nature* **310** 393
- [15] Ponyatovsky E G and Pozdnyakova T A 1995 *J. Non-Cryst. Solids* **188** 1153
- [16] Chakraverty B K 1969 *J. Phys. Chem. Solids* **30** 454
- [17] Regel A R and Glazov V M 1983 *Sov. Phys.–Semicond.* **17** 1105
- [18] Ponyatovsky E G 1958 *Dokl. Akad. Nauk* **120** 1021  
Apetkar I L and Ponyatovsky E G 1967 *Dokl. Akad. Nauk* **173** 852 (in Russian)
- [19] Ponyatovskii E G *et al* 1994 *JETP Lett.* **60** 360
- [20] Vaidya S N 1984 *Phys. Status Solidi a* **86** 565  
Vaidya S N 1985 *Phys. Status Solidi a* **87** 181  
Vaidya S N 1985 *Phys. Status Solidi a* **91** 37
- [21] Antonov V E *et al* 1993 *J. Alloys Compounds* **194** 279